Heat Flow and Hydrologic Characteristics at the AND-1B borehole, ANDRILL McMurdo Ice Shelf Project, Antarctica

Roger H. Morin*
United States Geological Survey, Mail Stop 403, Denver Federal Center, Denver, Colorado 80225, USA

Trevor Williams*
Lamont-Doherty Earth Observatory, Columbia University, Palisades, New York 10964, USA

Stuart A. Henrys*
Geological and Nuclear Sciences, P.O. Box 30 368, Lower Hutt, New Zealand

Diana Magens*
Frank Niessen*
Alfred Wegener Institute for Polar and Marine Research, Department of Marine Geophysics, Postfach 12 01 61, D-27515 Bremerhaven, Germany

Dhiresh Hansaraj*
Victoria University of Wellington, School of Earth Sciences, P.O. Box 600, Wellington, New Zealand

ABSTRACT

The Antarctic Drilling Program (ANDRILL) successfully drilled and cored a borehole, AND-1B, beneath the McMurdo Ice Shelf and into a flexural moat basin that surrounds Ross Island. Total drilling depth reached 1285 m below seafloor (mbsf) with 98 percent core recovery for the detailed study of glacier dynamics. With the goal of obtaining complementary information regarding heat flow and permeability, which is vital to understanding the nature of marine hydrogeologic systems, a succession of three temperature logs was recorded over a five-day span to monitor the gradual thermal recovery toward equilibrium conditions. These data were extrapolated to true, undisturbed temperatures, and they define a linear geothermal gradient of 76.7 K/km from the seafloor to 647 mbsf. Bulk thermal conductivities of the sedimentary rocks were derived from empirical mixing models and density measurements performed on core, and an average value of 1.5 W/mK ± 10 percent was determined. The corresponding estimate of heat flow at this site is 115 mW/m^2. This value is relatively high but is consistent with other elevated heat-flow data associated with the Erebus Volcanic Province. Information regarding the origin and frequency of pathways for subsurface fluid flow is gleaned from drillers' records, complementary geophysical logs, and core descriptions. Only two prominent permeable zones are identified and these correspond to two markedly different features within the rift basin; one is a distinct lithostratigraphic subunit consisting of a thin lava flow and the other is a heavily fractured interval within a single thick subunit.

INTRODUCTION

During the austral summer of 2006–2007, the Antarctic Drilling Program (ANDRILL) successfully drilled a borehole, AND-1B, beneath the McMurdo Ice Shelf (Naish et al., 2007a). The ice cover was ~82 m thick and water depth was 855 m. Total depth of the borehole reached 1285 m below seafloor (mbsf) with 98 percent core recovery of sedimentary rocks for detailed study of climate and ice-sheet dynamics (Naish et al., 2007b). The drillsite was situated on the northwest corner of the Ross Ice Shelf, ~9 km southeast of Hut Point Peninsula (Fig. 1), and above a flexural moat basin that surrounds Ross Island (Horgan et al., 2005). This basin was formed by loading of the crust from the basaltic volcanoes that constitute Ross Island within the tectonic framework of the Victoria Land Basin, a region of late Cenozoic crustal extension of the West Antarctic Rift System (e.g., Wilson, 1999; Hall et al., 2007; Henrys et al., 2007). Characterizing the marine hydrogeology at this site requires an understanding of fine-scale heat-flow patterns and structural details in order to evaluate moat-wide circulation processes, thermal refraction along the volcanic edifice, and channelized fluid flow (Harris et al., 2000a, 2000b).

A comprehensive downhole measurements program was devised for this borehole to complement ANDRILL's scientific objectives (Naish et al., 2006), and activities included the acquisition of numerous geophysical logs and vertical seismic profiles. Morin et al. (2007) present a detailed summary of logging operations that includes the technical specifications for logging tools. As part of the effort to contribute to the sparse heat-flow database for the region and gain additional insight into fluid-transport processes associated with these sub-basin environments, several of the geophysical logs are analyzed to quantify heat flow at this site and to investigate the hydrologic properties of the

*Emails: Morin: rhmorin@usgs.gov; Williams: trevor@ldeo.columbia.edu; Henrys: s.henrys@gns.cri.nz; Magens: diana.magens@awi.de; Niessen: frank.niessen@awi.de; Hansaraj: dhireshh@gmail.com.

Geosphere; August 2010; v. 6; no. 4; p. 370–378; doi: 10.1130/GES00512.1; 7 figures; 1 table.

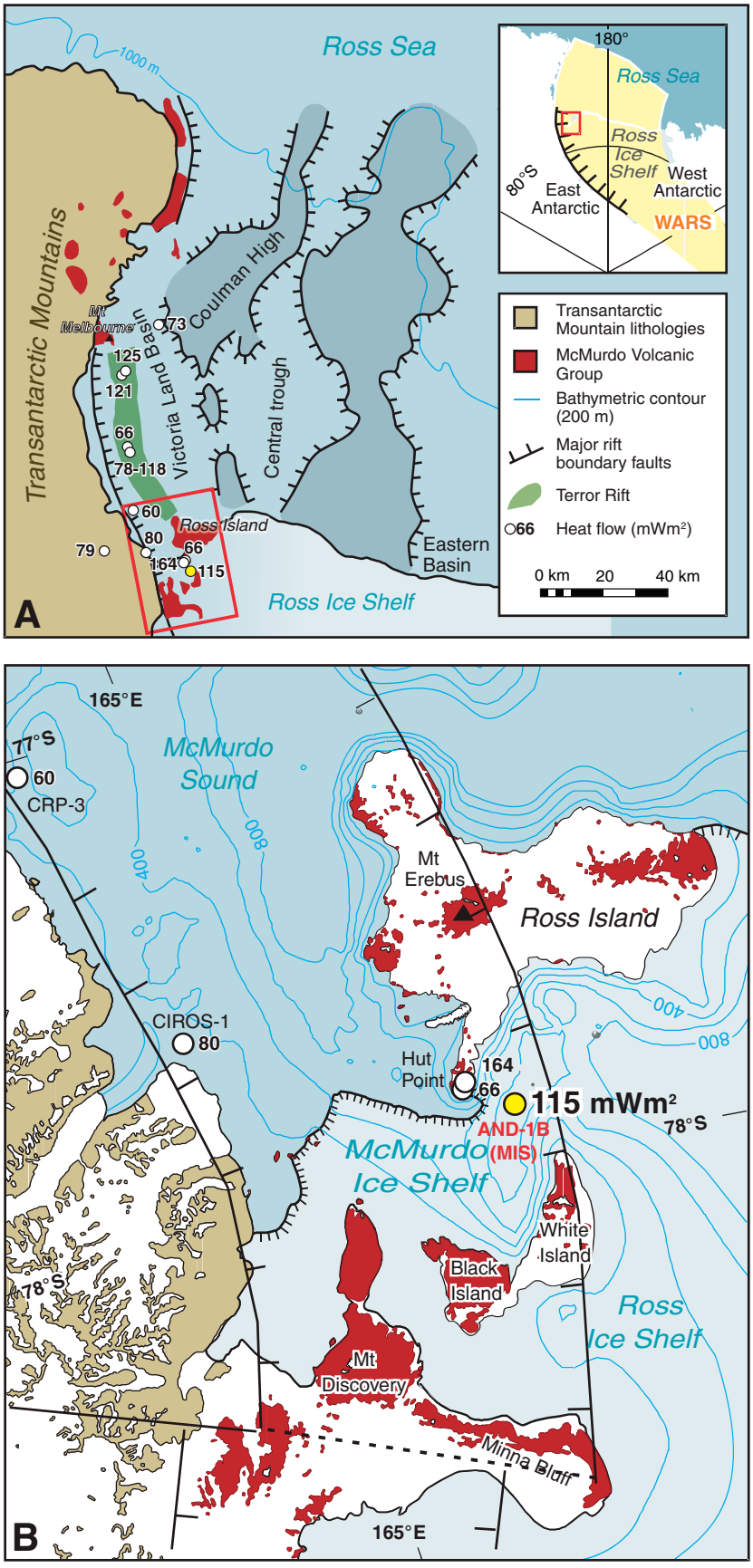

sedimentary rocks. Specifically, these measurements consist of three sequential temperature profiles as well as caliper, formation resistivity, acoustic televiewer and natural-gamma logs. Selected physical properties measured on core (Niessen et al., 2007) and detailed descriptions of core (Krissek et al., 2007) are also utilized to aid in the analyses.

TEMPERATURE LOGS AND GEOTHERMAL GRADIENT

The ambitious ANDRILL program of drilling and coring lasted for ~60 d at the AND-1 site. A PQ drillpipe (85.0 mm inside diameter – I.D.) was used to a depth of 238 mbsf, followed by a HQ drillpipe (63.5 mm I.D.) to 702 mbsf and a NQ drillpipe (47.6 mm I.D.) to the total depth of 1285 mbsf (Falconer et al., 2007). Drilling fluid consisted primarily of seawater mixed with potassium chloride and polymers. Once these operations were concluded, the borehole was made available for downhole measurements. However, these in situ measurements could only reach a depth of ~1000 mbsf because of the length limitations of the logging cable.

Geophysical logs included a succession of three temperature logs recorded over a span of 5 d; these are illustrated in Figure 2 with an expanded view across a 100-m section shown in Figure 3. A natural-gamma log, stacked and corrected for signal attenuation through the drillpipe, is also presented for lithologic reference (Williams et al., 2008). The temperature sensor housed within the logging tool has a resolution of 0.007 °C. Due to extensive bridging in an unstable borehole at the start of logging operations, a NQ drillpipe was lowered into the open hole below the base of the HQ drillpipe (set at 690 mbsf from the original 702 mbsf) in order to permit access with logging tools. The

Figure 1. (A) Ross Sea rift basins and Transantarctic Moutains are components of the West Antarctic Rift System (WARS – inset). Heat flow measurements made in the Victoria Land Basin are annotated and shown by white filled circles (see Table 1 for references). Within the Victoria Land Basin the Terror Rift, a 70-km-wide structure extending from Mt. Erebus to Mt. Melbourne, has been identified as the zone of most recent deformation (Cooper et al., 1987; Salvini et al., 1997). (B) Detailed map of Southern McMurdo Sound showing the location of the McMurdo Ice Shelf (MIS) drill hole AND-1B (yellow filled circle) and its heat flow value at the southern end of Terror Rift.

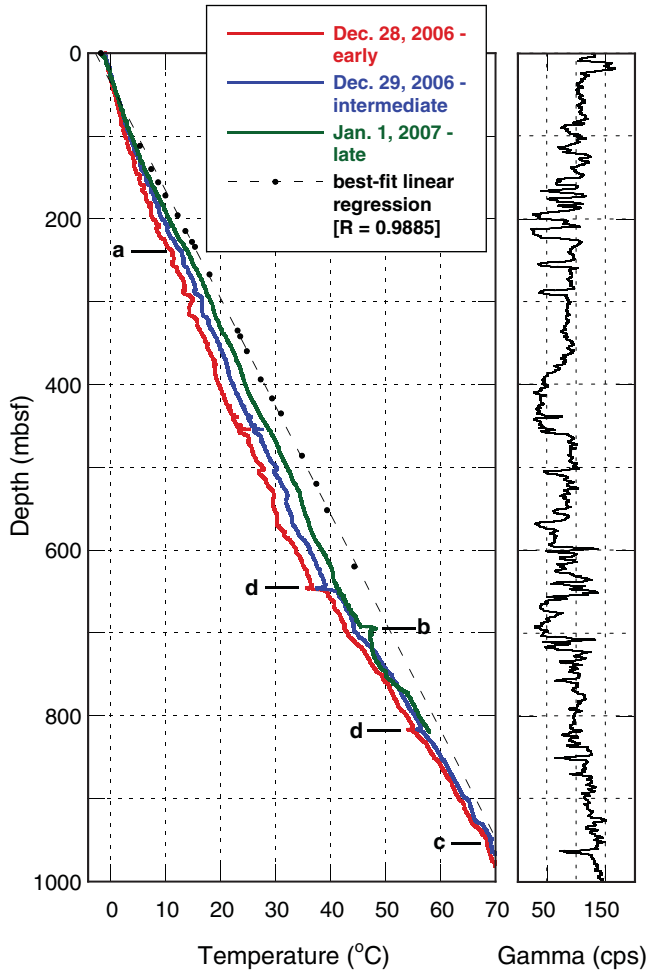

Figure 2. Time sequence of three temperature logs and extrapolated data points with best-fit linear regression. (A) indicates base of PQ drillpipe, (B) base of HQ drillpipe, (C) base of NQ drillpipe during first temperature log; it was later retracted for remaining two temperature logs, and (D) zones of lost mud circulation. Natural-gamma log is included for lithologic reference (Williams et al., 2008).

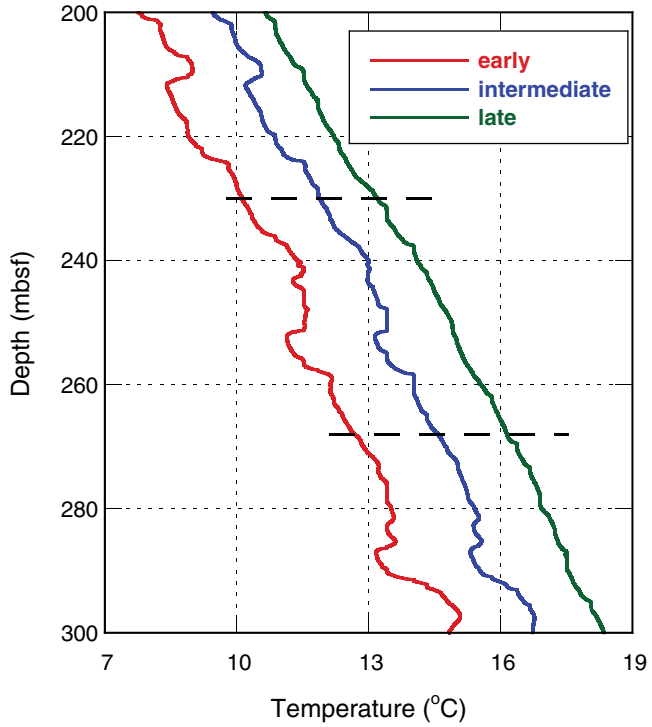

Figure 3. Expanded view of temperature logs across 100-m section. Horizontal dashed lines identify selected depths where temperature logs display a smooth transition between profiles and where data points were utilized to compute true temperature.

first temperature log collected on 28 December 2006 was run inside this pipe. The second log was recorded ~11 h later after the NQ pipe had been retracted and the open hole remained stable. The last temperature log was recorded 3 d after this second one on 1 January 2007, but the logging tool could only be lowered to a depth of 816 mbsf before encountering an obstruction that prevented it from descending further. All three logs consistently registered a temperature at the seafloor of −1.68 °C, a value that is in good agreement with hydrographic data obtained from the water column at nearby locations that indicate bottom-water temperatures of about −1.89 °C (Barrett et al., 2005).

In general, the three successive temperature logs (early, intermediate, and late time) depict a fairly rapid rebound toward equilibrium geothermal conditions, possibly an effect of relatively small borehole diameters that restrict initial cooling (Langseth, 1990). The profiles are interspersed with sharp anomalies that typically dissipate over time and may no longer be apparent in the late temperature record (Fig. 3). These small drifts in temperature may represent instances of transient fluid exchange between the borehole and the formation (e.g., Drury et al., 1984; Ge, 1998; Šafanda et al., 2007) or localized intervals of fluid convection within the borehole (e.g., Diment, 1967; Fisher and Becker, 1991). Substantial thermal anomalies appear at 647 mbsf, a consequence of circulation loss and drilling fluid entering the surrounding formation within a fracture zone delineated by a thin lava flow (Falconer et al., 2007; Krissek et al., 2007). Below this depth, the temperature profiles do not recover sufficiently from this fluid invasion to follow a clear and systematic return to thermal equilibrium over a 5-d period. Moreover, the borehole is open below 690 mbsf and temperatures are more susceptible to disturbances caused by subtle fluid movement between permeable zones that is not hindered by the presence of drillpipe. Therefore, the following examination of temperature re-equilibration with time is confined to the uppermost part of the borehole between the seafloor and 647 mbsf.

The three temperature records obtained across this interval are analyzed to arrive at values of the true, undisturbed temperature at selected depths in the borehole from which an overall estimate for the background geothermal gradient can be determined for this site. Specific depths were chosen where the temperatures displayed a relatively smooth transition between successive profiles and where extraneous thermal disturbances appeared to be minimal; two examples of these locations are depicted as horizontal dashed lines in Figure 3. There are numerous techniques for extrapolating a series of transient temperature records to infinite recovery time, thereby computing the true formation temperature from in situ measurements. Hermanrud et al. (1990), for example, present an overview of 22 different methods along with their underlying assumptions. Of these, the line-source method of Horner (1951), as implemented by Lachenbruch and Brewer (1959), is relatively precise even though it does contain an inherent bias to lower temperatures that reduces accuracy slightly (Beardsmore and Cull, 2001). A detailed study describing the proper application of this method has recently been reported by He et al. (2008).

In this method, a Horner plot is constructed from the following expression using temperature data obtained at any particular depth z:

$$T_{log} = T_{true} + [(Q/4\pi\lambda)] * 1n[1 + (t_{dc}/\Delta t)], \quad (1)$$

where T_{log} = downhole temperature obtained from temperature log (°C), T_{true} = true formation temperature (°C), Q = rate at which heat is being supplied to the borehole (W/m), λ = thermal conductivity of surrounding rocks at depth z (W/mK), Δt = time elapsed from cessation of mud circulation to actual measurement (hr), and t_{dc} = time elapsed between end of drilling and end of mud circulation (hr). Data from the three temperature profiles shown in Figure 2 and corresponding to three depths are presented in Figure 4 in the form of a Horner plot. Temperature is plotted versus the logarithmic term in Equation (1), and it is not required that the parameters Q and λ be known. A linear best-fit is drawn through the points and its intercept at the y-axis represents the true formation temperature at infinite recovery time ($\Delta t = \infty$).

The true temperature at each depth is based upon the spread of three points from which a regression line is constructed and a correlation coefficient determined. In this ANDRILL case, having three points (three temperature logs) instead of only two greatly reduces the uncertainty of this technique (e.g., Kreyszig, 1983). However, estimating values for Δt and t_{dc} is problematic because some drillsite operations that continued after drilling and coring had formally ceased may have produced disturbances to the borehole fluid and the thermal environment. These activities included intermittent circulation of drilling fluid to wash the borehole wall in preparation for acoustic televiewer logging, efforts to clear obstructions in the open hole below the base of the HQ drillpipe, and attempts at cutting the HQ drillpipe (Falconer et al., 2007). Consequently, values of Δt and t_{dc} are approximate and contribute to any error in

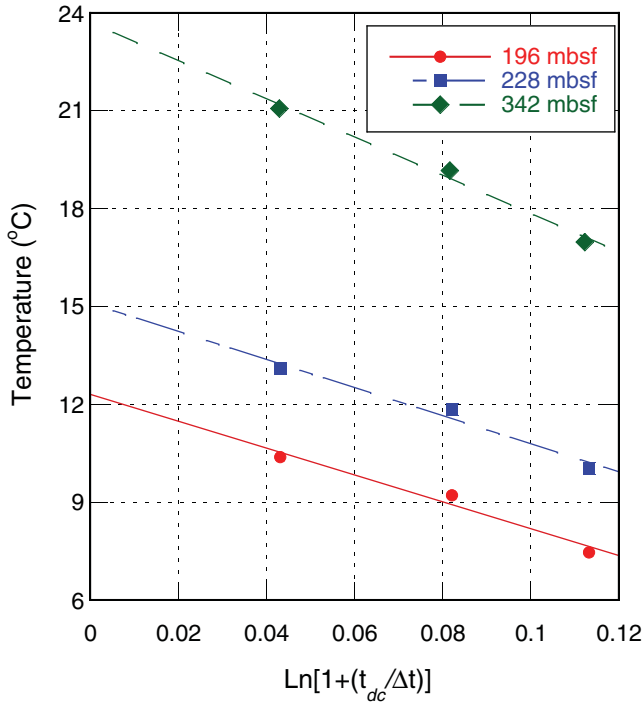

Figure 4. Horner plot showing best-fit linear regression to three temperature values recorded at different times for each of three depths. Intercept at Y-axis denotes true temperature at infinite recovery time ($\Delta t = \infty$).

estimating T_{true}. However, their placement in the logarithmic term of Equation (1) and their eventual use in the best-fit approximation of the Horner method tend to diminish this uncertainty.

A total of 19 depths were selected in which the three temperature records displayed a smooth transition from one profile to the next, as illustrated in Figure 3; the extrapolated values of the true temperatures are plotted as solid points in Figure 2. A regression line drawn through all points intercepts the seafloor at a temperature of −2.4 °C and represents the temperature distribution as a function of depth in this borehole (correlation coefficient R = 0.988). This exercise defines a linear geothermal gradient of 76.7 K/km at this site. An estimation of the temperature gradient between each two adjacent points and across the depth interval between them is presented in Figure 5A, where deviations from the average value (vertical dashed line) reflect variations in the bulk thermal conductivity of the surrounding rocks. Coincidently, a natural-gamma log is presented in Figure 5C to illustrate lithologic variability. For comparison, Bücker et al. (2001) present a compilation of geothermal-gradient data for the Transantarctic Mountains and Victoria Land Basin, with values ranging from 24 to 80 K/km.

THERMAL CONDUCTIVITY AND HEAT FLOW

Thermal conductivity was not directly measured on core samples from the AND-1B borehole. Referring to Equation (1) and the Horner plots (Fig. 4), λ is indeterminable from the slope of the regression line because Q is unknown. As an alternative method, Lee et al. (2003) proposed a finite-element solution for deriving the thermal conductivity of rocks from borehole thermal-recovery data. Jones and Pascal (1994) developed a numerical model that considers the effects of grain size and orientation on the thermal conductivity of composites. For our purposes, however, values of thermal conductivity, λ, are more effectively estimated from empirical mixing models of components and evaluated against data reported for comparable sedimentary rocks.

Numerous mixing models have been proposed to compute the thermal conductivity of sediment mixtures based upon packing arrangements and particle geometries among matrix components (e.g., Birch and Clark, 1940; Hashin and Shtrikman, 1962; Crane and Vachon, 1977; Pribnow and Sass, 1995). These can be broadly separated into a few categories (e.g., Beardsmore and Cull, 2001): (1) harmonic mean or series combination, (2) arithmetic mean or parallel combination, (3) geometric mean or random mixture, and (4) square-root mean. We prefer to use either category (3) or (4) because of the nature of the rocks encountered in this borehole, where particles are most likely to be randomly orientated and distributed (Pompilio et al., 2007). Some investigators (e.g., Woodside and Messmer, 1961; Lovell, 1985; Vasseur et al., 1995) have concluded that the geometric-mean model (3) is adequate for predicting experimental data. Roy et al. (1981), on the other hand, preferred the square-root mean model (4), arguing that it was derived from stronger physical principles than the others.

The geometric-mean model, in general terms, is:

$$\lambda_b = \prod_{i=1}^{n} \lambda_i^{v_i}, \qquad (2)$$

where λ_b = bulk thermal conductivity of mixture (W/mK), λ_i = thermal conductivity of component i (W/mK), and v_i = volume fraction of component i (dimensionless). In order to accurately apply Equation (2) to compute λ_b, the mineral composition of the sedimentary rocks must be known. Core descriptions (Krissek et al., 2007) identify 16 separate lithostratigraphic subunits that extend from the seafloor to 647 mbsf and consist of varying amounts of diamictite, mudstone, sandstone, and diatomite, among other constituents. Rather than assigning a value of thermal conductivity for each mineral associated with these deposits, we assume that the solid fraction of the sediment mixture can be represented by a single value for the thermal conductivity of the grains.

Thus, the geometric-mean expression for a saturated and isotropic binary mixture of grains and seawater reduces to:

$$\lambda_b = \lambda_g^{1-\phi} \lambda_f^{\phi}, \qquad (3)$$

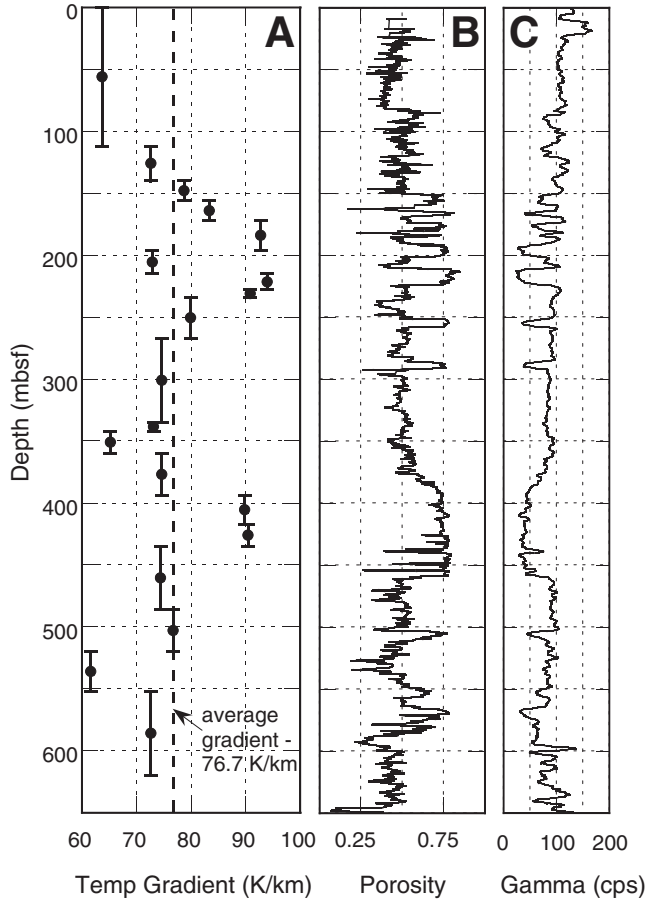

Figure 5. (A) Vertical distribution of thermal gradients between adjacent temperature values and across depth intervals. Vertical dashed line depicts average thermal gradient for entire borehole. (B) Sedimentary rock porosities with respect to depth as computed from density measurements performed on core (Niessen et al., 2007). (C) Natural-gamma log included for lithologic reference (Williams et al., 2008).

where λ_g = thermal conductivity of solid grains (W/mK), λ_f = thermal conductivity of fluid, in this case seawater (W/mK), and Φ = porosity (dimensionless). Also, under these assumptions, the square-root mean relation is:

$$\sqrt{\lambda_b} = \left\{(1-\phi)\sqrt{\lambda_g}\right\} + \left\{\phi\sqrt{\lambda_f}\right\}. \quad (4)$$

A representative value for λ_g can be constrained by examining similar analyses of thermal conductivity performed for comparable sedimentary rocks and marine sediments. As part of the Cape Roberts Drilling Project based at the western edge of the Victoria Land Basin, a heat-flow study conducted by Bücker et al. (2001) consisted of recording borehole temperatures in Hole CRP-3 and measuring the thermal conductivity of core samples. An average bulk thermal conductivity was determined to be 2.1 W/mK. Many of the lithologic units identified in the Hole CRP-3 (Powell et al., 2001) are similar to those encountered in the AND-1B borehole, though porosities appear to be generally lower and average ~0.25 (Jarrard, 2001). Substituting these values of λ_b and Φ into Equations (3) and (4) yields estimates for the grain thermal conductivity, λ_g, that range from 2.8 to 3.2 W/mK and are mainly a function of quartz content. These values are in good agreement with those reported by Villinger et al. (1994) for marine sediments, where values of λ_g between 2.6 and 3.2 W/mK were found to predict temperature profiles accurately. Consequently, we use this range of values for the grain thermal conductivity (2.8 - 3.2 W/mK) in our computation of bulk thermal conductivity for AND-1 sedimentary rocks.

Sediment porosities, as illustrated in Figure 5B, are computed from density measurements performed on core (Niessen et al., 2007) and have an average value of ~0.50 across the uppermost 650 m. The sedimentary rocks having the highest porosities are the diatomites, due to the hollow nature of diatom frustules. These are clearly delineated in the natural-gamma log (Fig. 5C), where high radiation values generally correspond to sub-glacial diamictite and low values to open-water diatomites (Williams et al., 2008). The diatomites also have the lowest quartz content.

Assuming that the vertical flow of heat through the ocean floor remains constant, variations in porosity with respect to depth tend to mimic the vertical distribution of the temperature gradient (Fig. 5). Conversely, the profile of bulk thermal conductivity, λ_b, which is negatively correlated to porosity, mirrors that of the temperature gradient. With Φ equal to 0.50 and λ_g ranging between 2.8 and 3.2 W/mK, the geometric-mean model (Equation 3) and the square-root mean model (Equation 4) yield an average value for λ_b of 1.5 W/mK ± 10 percent. The estimates of bulk thermal conductivity for sandstones and siltstones in this borehole are slightly lower than those reported by Bücker et al. (2001) for similar sedimentary rocks because of generally lower porosities encountered at Hole CRP-3 (Jarrard, 2001). Correspondingly, estimates of thermal conductivity for diatomites are generally higher than those reported for marine siliceous oozes (Morin and Silva, 1984; Lovell, 1985) because diatomite porosities are substantially lower. Therefore, once adjustments are made for differences in porosity, values of λ_b in the AND-1B borehole are comparable to other reported values.

It should be noted that the thermal conductivities of the grains and of seawater are also dependent upon temperature. Since in situ temperatures reached 70 °C at a depth of ~1000 mbsf (Fig. 2), changes in these constituent conductivities are expected. However, a slight increase in the thermal conductivity of seawater (Lawson et al., 1959; Yusufova et al., 1978) with increasing temperature is counteracted by a slight decrease in the value of λ_g (Birch and Clark, 1940; Sass et al., 1992). Given the relative error in the estimation of λ_g, the uncertainty related to temperature effects is negligible.

The product of this average value of bulk thermal conductivity and the best-fit linear geothermal gradient yields an estimate of 115 mW/m^2 for the heat flow at this site (Fig. 1B). This value is higher than most heat-flow measurements reported along the margin of the Victoria Land Basin (Blackman et al., 1987; Bücker et al., 2001), but is consistent with the elevated heat flow (Sato et al., 1984; Della Vedova et al., 1992) associated with the McMurdo Volcanic Group, Erebus Volcanic Province (Kyle, 1990), and Terror Rift (Cooper et al., 1987; Salvini et al., 1997). The spatial distribution of heat-flow values for the region is displayed in Figure 1A and summarized in Table 1.

The high heat flow may be a direct manifestation of a thermal anomaly within the upper mantle and beneath Ross Island (Watson et al., 2006), and also is typical of the effects of crustal extension and thinning on temperatures within rift basins (Jaupart and Mareschal, 2007). For example, high heat flow values greater than

TABLE 1. SUMMARY OF HEAT FLOW MEASUREMENTS REPORTED FOR THE VICTORIA LAND BASIN AND TRANSANTARCTIC MOUNTAINS

Latitude	Longitude	Station #	Water Depth (m)	Temperature Gradient (K/km)	Heat flow (mW/m^2)	Reference
-75°01'15"	165°55'10"	1	1020	93.5 ± 4.6	125	Della Vedova et al. (1992)
-75°03'22"	165°42'28"	2	1032	94.6 ± 2.1	121	Della Vedova et al. (1992)
-76°07'18"	165°07'18"	4	865	76.6 ± 6.6	100	Della Vedova et al. (1992)
-76°09'50"	165°05'36"	5	870	83.1 ± 1.1	91	Della Vedova et al. (1992)
-76°09'40"	165°04'19"	6	870	109.4 ± 2.6	98	Della Vedova et al. (1992)
-76°06'17"	164°59'16"	7	885	71.9 ± 0.5	78	Della Vedova et al. (1992)
-76°06'25"	164°59'09"	8	875	99.1 ± 4.4	103	Della Vedova et al. (1992)
-76°02'36"	164°59'18"	9	875	91.4 ± 9.0	87	Della Vedova et al. (1992)
-76°02'33"	165°00'14"	10	880	87.8 ± 3.9	100	Della Vedova et al. (1992)
-76°02'54"	164°53'33"	11	885	88. 1 ± 3.7	105	Della Vedova et al. (1992)
-76°03'00"	164°54'54"	12	893	123.2 ± 23.5	118	Della Vedova et al. (1992)
-76°04'00"	164°53'00"	6	912	98 ± 6	66	Blackman et al. (1987)
-74°29'00"	168°10'00"	9	909	108 ± 10	73	Blackman et al. (1987)
		Drill hole	Drill hole depth (mbsf)			
-77°49'48"	166°40'30"	Hut Point	7.6	79.7 ± 18	164	Risk and Hochstein (1974)
-77°51'00"	166°40'29"	DVDP-3	90-260	36.3	**66**	Decker and Bücher (1982)
-77°22'48"	161°48'37"	DVDP-6	10-305	31	**79**	Decker and Bücher (1982)
-77°00'01"	163°38'25.4"	CRP-3	20-920	28.5	**60**	Bücker et al. (2001)
-77°34'55"	164°29'55.9"	CIROS-1	280-450	40	**80**	White (1989)
-77°53'22"	167°05'21.6"	AND-1B	0-647	76.7	**115**	This paper

Note: The most reliable determinations are from repeat temperature logs recorded in deep boreholes, shown in boldface type. Marine heat flow measurements were determined using a temperature probe. A heat flow value of 80 mW/m^2 at CIROS-1 assumed a thermal conductivity of 2.0 W/mK.

110 mW/m^2 have been reported for the Basin and Range Province in southwestern United States (Sass et al., 1994). These are not uncommon and are directly attributable to rapid rifting processes. The heat flow measured at the AND-1B borehole may also be directly affected by hydrothermal circulation sustained through recharge and discharge along the nearby volcanic edifice; this effect would not be prominent along the margin of the Victoria Land Basin.

ATTENDANT GEOPHYSICAL LOGS AND HYDROLOGIC PROPERTIES

Because plans to run straddle-packer tests (Naish et al., 2006) were not implemented during this project, no in situ measurements of hydraulic conductivity (e.g., Becker and Davis, 2004) were made in this borehole and no values of this property can be accurately assigned to various lithostratigraphic units. Nevertheless, information regarding the nature and frequency of permeable zones within the sedimentary moat may be gleaned from drillers' records of lost circulation of drilling fluid into the formation combined with supplemental downhole data. Falconer et al. (2007) noted only two instances of significant loss of circulation, and these were later confirmed from reviewing detailed records of fluid pumping and corresponding return rates at the drill rig. These zones appear (1) at 647 mbsf corresponding to a thin lava flow, and (2) at 815 mbsf where return of drilling fluid was completely lost and never totally regained for the remainder of drilling and coring operations. Both of these permeable zones are delineated by conspicuous shifts in the temperature logs (Fig. 2).

The upper permeable zone (647 mbsf) was cased with HQ drillpipe and remained so during all phases of geophysical logging. Consequently, no acoustic televiewer logs (Zemanek et al., 1970) could be obtained across this section to inspect the borehole wall visually. However, this depth corresponds to a major lithostratigraphic subunit LSU 5.2 (Krissek et al., 2007) that is also reflected in a marked shift in the natural gamma log (Morin et al., 2007). LSU 5.2 is composed of a 2.8-m-thick phonolitic lava with tiny shear fractures related to the early stages of cooling and larger voids related to viscous flow and ductile-brittle transition during the later stages of lava formation (M. Pompilio, 2009, personal commun.); a split-core photo of this rock is shown in Figure 6A. These fractures and voids likely account for the loss of circulation and high permeability at this depth.

The lower permeable zone (815 mbsf) is within the 139-m thick lithostratigraphic subunit (LSU 6.1) that extends from 759.32 to 897.95 mbsf, and consists of a range of different lithologies including mudstone, diamictite, sandstone and conglomerate/sandy breccia (Krissek et al., 2007). It is located in the open-hole section below the base of the HQ drillpipe and was accessible for logging with the acoustic televiewer. The magnetically oriented image of the borehole wall at this depth, corrected for local magnetic declination, is presented in Figure 7 alongside coincident profiles of caliper, early temperature, formation resistivity (induction), and natural-gamma activity. A large fracture, washed out to a width of almost 1 m at the borehole, is detected in both the televiewer and caliper logs that strikes approximately east-west and dips roughly 60° to the north. A split-core photo of the rock just below this interval is shown in Figure 6B. The rock is highly fractured, with a missing section from 816.48 to 816.64 mbsf, and no core recovery from 816.82 to 819.19 mbsf. Considering uncertainties in the depth correlation between downhole measurements and drillers' depths (roughly +/– 1 m) due to a combination of factors such as cable stretch, pipe stretch, and a possible error in the circumference of the encoder wheel from which cable depth is determined (Morin et al., 2007), the marked absence of core likely corresponds to the large gap in the televiewer image and

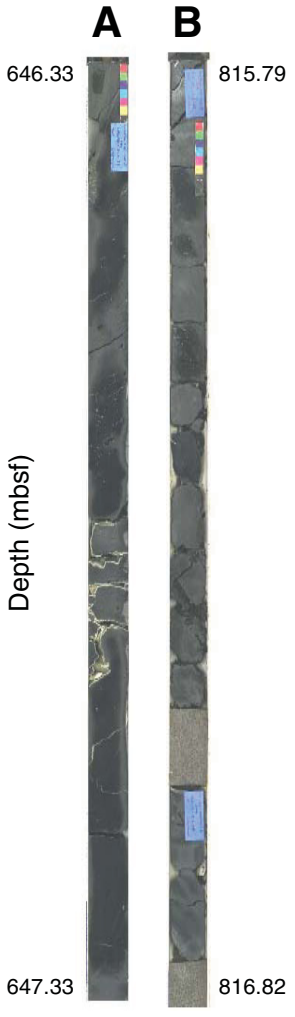

Figure 6. Split-core photos of rocks recovered from (A) 646.33–647.33 mbsf and (B) 815.79–816.82 mbsf.

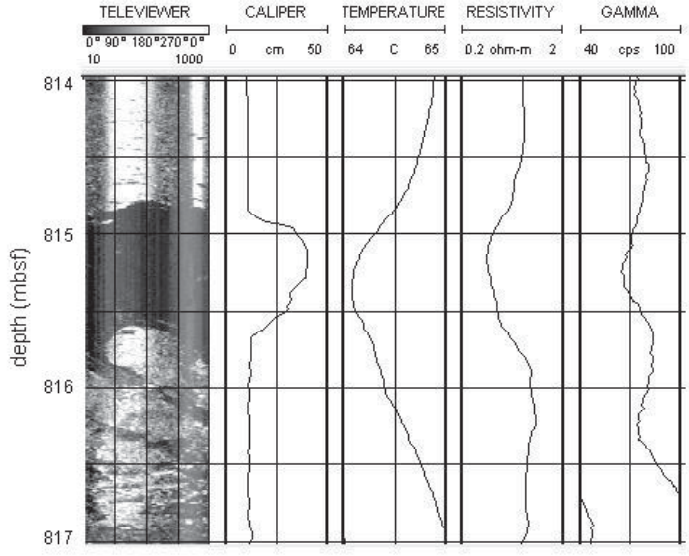

Figure 7. Geophysical log composite across a 3-m depth interval showing magnetically oriented, acoustic televiewer image of borehole wall with prominent fracture alongside coincident caliper, early temperature, formation resistivity, and natural gamma profiles.

identifies the source of circulation loss. Slight decreases in the natural gamma and resistivity logs at a depth corresponding to this prominent fracture (Fig. 7) indicate a lack of material (caliper log) needed to generate a signal.

Regrettably, neither permeable zone can be clearly recognized from the surface seismic records; the upper lava flow because it is too thin and the lower fractured interval because of its lack of contrast in physical properties within a thick lithostratigraphic subunit. Consequently, their lateral extents cannot be extrapolated to a larger scale to help develop a conceptual model of moat hydrology and basin fluid-transport. Based upon depositional processes and conditions, the lava flow is probably a local feature (not basin wide) that extends for perhaps several km in length but narrower in width (M. Pompilio, 2009, personal commun.). However, the deeper permeable zone is characterized by a section of heavily fractured rocks that may represent a fault and thereby imply the presence of a broader hydrologic system. Several investigators have reported evidence of channelized water circulation in the oceanic lithosphere (Fisher and Becker, 2000; Géli et al., 2008), where hydrogeological processes may be affected by a variety of factors such as distribution and thickness of sediment cover, location of outcrops, bedrock topography, and spatial distribution of permeability (Davis and Elderfield, 2004). Closely spaced heat-flow data may also help delineate wavelengths and constrain the geometry of circulation cells (e.g., Fisher and Becker, 1995; Harris and McNutt, 2007). However, reliable heat-flow measurements are too sparse within the southern Victoria Land Basin (see Figure 1 and Table 1) to provide the type of fine-scale resolution required to construct realistic submarine hydrogeological models (e.g., Harris et al., 2000b).

CONCLUSIONS

Data from three temperature logs recorded over a span of 5 d in the AND-1B borehole were extrapolated to true, undisturbed temperatures; the corresponding thermal gradient from the seafloor to 647 mbsf was determined to be 76.7 K/km at this site. An average value of thermal conductivity for the sedimentary rocks was computed from empirical mixing models constrained to a narrow range of possible constituent thermal conductivities. Profiles of temperature gradient and sediment porosity tend to parallel each other as the thermal conductivity responds inversely to porosity. The corresponding heat flow is estimated to be 115 mW/m^2. Although this magnitude of heat flow is higher than typically reported for the Victoria Land Basin on a regional scale, it is in good agreement with more local measurements associated with the Erebus Volcanic Province and its elevated thermal anomaly. Heat-flow values that exceed roughly 100 mW/m^2 are common for the Terror Rift and appear to be a direct manifestation of its most recent deformation with crustal thinning and extension.

Two dominant pathways for subsurface fluid flow are identified and these correspond to two markedly different features within the rift subbasin: (1) a distinct lithostratigraphic subunit consisting of a thin lava flow, and (2) a heavily fractured interval within a single thick subunit. Additional, but less prominent, transmissive zones may also exist as perhaps suggested by several subtle disturbances to the temperature profiles (e.g., Ge, 1998; Birkholzer, 2006) and by drillers' records that indicate slight and sporadic loss of circulation. However, these two zones probably represent the major pathways for fluid flow intercepted by this borehole. Regrettably, their spatial extents are not well constrained, and insight into general hydrologic characteristics cannot be extrapolated to a basin scale that includes a flexural moat and a volcanic edifice.

Coupled heat-transport and fluid-flow processes are expected to be vigorous near Ross Island due to crustal extension and thinning combined with permeable zones located both at lithologic contacts and within lithostratigraphic subunits. However, reliable heat-flow data are sparse in this area and hydrogeologic simulations that provide important insight into the thermal regime require fine-scale, high-resolution measurements. Nevertheless, these new results determined from geophysical logs collected in the AND-1B drillhole provide high-quality data that may be integrated into this regional database.

ACKNOWLEDGMENTS

The authors are grateful to C. Bücker, R. Saltus, Guest Associate Editor T. Paulsen, and an anonymous reviewer for their thorough and thoughtful reviews that improved this manuscript considerably. ANDRILL is a multinational collaboration among the Antarctic programs of Germany, Italy, New Zealand, and the United States. The authors would also like to thank the project operator, Antarctica New Zealand, and Alex Pyne at Victoria University of Wellington, along with the drilling crew of Webster Drilling and Enterprises Ltd. for their tireless and conscientious support at the drillsite that enabled geophysical logs to be collected. This material is based upon work supported by the National Science Foundation under Cooperative Agreement No. 0342484 through sub-awards administered by the ANDRILL Science Management Office at the University of Nebraska–Lincoln, and issued through Northern Illinois University, as part of the ANDRILL U.S. Science Support Program. Any opinions, findings, and conclusions or recommendations expressed in this material are those of the authors and do not necessarily reflect the views of the National Science Foundation. Support for SAH and DH was provided by New Zealand Foundation for Research Science and Technology and the Royal Society of New Zealand Marsden.

REFERENCES CITED

Barrett, P.J., Carter, L., Dunbar, G.B., Dunker, E., Giorgetti, G., Harper, M.A., McKay, R.M., Niessen, F., Nixdorf, U., Pyne, A.R., Riesselmann, C., Robinson, N., Hollis, C., and Strong, P., 2005, Oceanography and sedimentation beneath the McMurdo Ice Shelf in Windless Bight, Antarctica, Antarctic Data Series 25, Antarctic Research Centre, Victoria University of Wellington, 100 p.

Beardsmore, G.R., and Cull, J.P., 2001, Crustal Heat Flow: A Guide to Measurement and Modelling: Cambridge, UK, Cambridge University Press, 324 p.

Becker, K., and Davis, E.E., 2004, In situ determinations of the permeability of the oceanic igneous crust, *in* E.E. Davis and H. Elderfield, eds., Hydrogeology of the Oceanic Lithosphere: New York, Cambridge University Press, p. 189–224.

Birch, F., and Clark, H., 1940, The thermal conductivity of rocks and its dependence upon temperature and composition: American Journal of Science, v. 238, no. 8, p. 529–635.

Birkholzer, J.T., 2006, Estimating liquid fluxes in thermally perturbed fractured rock using measured temperature profiles: Journal of Hydrology (Amsterdam), v. 327, p. 496–515, doi: 10.1016/j.jhydrol.2005.11.049.

Blackman, D.K., Von Herzen, R.P., and Lawver, L.A., 1987, Heat flow and tectonics in the western Ross Sea, Antarctica, *in* Cooper, A.K., and Davey, F.J., eds., The Antarctic Continental Margin: Geology and Geophysics of the Western Ross Sea: CPCEMR Earth Science Series, v. 5B: Houston, Texas, Circum-Pacific Council for Energy and Mineral Resources, p. 179–189.

Bücker, C.J., Jarrard, R.D., and Wonik, T., 2001, Downhole temperature, radiogenic heat production, and heat flow from the CRP-3 drillhole, Victoria Land Basin, Antarctica: Terra Antartica, v. 8, no. 3, p. 151–159.

Cooper, A.K., Davey, F.J., and Behrendt, J.C., 1987, Seismic stratigraphy and structure of the Victoria Land Basin, western Ross Sea, Antarctica, *in* Cooper, A.K., and Davey, F.J., eds., The Antarctic Continental Margin: Geology and Geophysics of the Western Ross Sea, CPCEMR Earth Science Series, v. 5B: Houston, Texas, Circum-Pacific Council for Energy and Mineral Resources, p. 27–66.

Crane, R.A., and Vachon, R.I., 1977, A prediction of the bounds on the effective thermal conductivity of granular materials: International Journal of Heat and Mass Transfer, v. 20, p. 711–723, doi: 10.1016/0017-9310(77)90169-7.

Davis, E.E., and Elderfield, H., eds., 2004, Hydrogeology of the Oceanic Lithosphere: New York, Cambridge University Press, 706 p.

Decker, E.R., and Bücker, C.J., 1982, Geothermal studies in the Ross Island-Dry Valley region: Madison, University of Wisconsin Press, p. 887–894.

Della Vedova, B., Pellis, G., and Lawver, L.A., 1992, Heat flow and active tectonics of the western Ross Sea, *in* Yoshida, Y., Kaminuma, K., and Shiraishi, K., eds., Proceedings of the 6th ISAES: Saitama, Japan, p. 627–637.

Diment, W.H., 1967, Thermal regime of a large diameter borehole: instability of the water column and comparison of air- and water-filled conditions: Geophysics, v. 32, p. 720–726, doi: 10.1190/1.1439885.

Drury, M.J., Jessop, A.M., and Lewis, T.J., 1984, The detection of ground-water flow by precise temperature measurements in boreholes: Geothermics, v. 13, no. 3, p. 163–174, doi: 10.1016/0375-6505(84)90013-0.

Falconer, T., Pyne, A., Levy, R., Olney, M., Curren, M., and the ANDRILL-MIS Science Team, 2007, Operations overview for the ANDRILL McMurdo Ice Shelf Project: Terra Antartica, v. 14, no. 3, p. 131–140.

Fisher, A.T., and Becker, K., 1991, The reduction of measured heat flow with depth in DSDP hole 504B: evidence for convection of borehole fluids?: Scientific Drilling, v. 2, p. 34–40.

Fisher, A.T., and Becker, K., 1995, Correlation between seafloor heat flow and basement relief: Observational and numerical examples and implications for upper crustal permeability: Journal of Geophysical Research, v. 100, p. 12,641–12,657, doi: 10.1029/95JB00315.

Fisher, A.T., and Becker, K., 2000, Channelized fluid flow reconciles heat-flow and permeability data: Nature, v. 403, p. 71–74, doi: 10.1038/47463.

Ge, S., 1998, Estimation of groundwater velocity in localized fracture zones from well temperature profiles: Journal of Volcanology and Geothermal Research, v. 84, p. 93–101, doi: 10.1016/S0377-0273(98)00032-8.

Géli, L., Lee, T.C., Cochran, J.R., Francheteau, J., Abbott, D., Labails, C., and Appriou, D., 2008, Heat flow from the Southeast Indian Ridge flanks between 80°E and 140°E: Data review and analysis: Journal of Geophysical Research, v. 113, no. B01101, p. 1–23, doi: 10.1029/2007JB005001.

Hall, J., Wilson, T., and Henrys, S., 2007, Structure of the central Terror Rift, western Ross Sea, Antarctica, *in* Cooper , A.K., and Raymond, C.R., eds., Antarctica: A Keystone in a Changing World—Online Proceedings of the 10th ISAES: USGS Open-File Report 2007–1047, Research Paper 108.

Harris, R.N., Von Herzen, R.P., McNutt, M.K., Garven, G., and Jordahl, K., 2000a, Submarine hydrogeology of the Hawaiian archipelagic apron 1. Heat flow patterns north of Oahu and Maro Reef: Journal of Geophysical Research, v. 105, no. B9, p. 21,353–21,369, doi: 10.1029/2000JB900165.

Harris, R.N., Garven, G., Georgen, J., McNutt, M.K., Christiansen, L., and Von Herzen, R.P., 2000b, Submarine hydrogeology of the Hawaiian archipelagic apron 2. Numerical simulations of coupled heat transport and fluid flow: Journal of Geophysical Research, v. 105, no. B9, p. 21,371–21,385, doi: 10.1029/2000JB900164.

Harris, R.N., and McNutt, M.K., 2007, Heat flow on hot spot swells: Evidence for fluid flow, Journal of Geophysical Research, v. 112, B03407, p. 1–14, doi:10.1029/2006JB004299.

Hashin, Z., and Shtrikman, S., 1962, A variational approach to the theory of the effective magnetic permeability of multiphase materials: Journal of Applied Physics, v. 33, p. 3125–3131, doi: 10.1063/1.1728579.

He, L., Hu, S., Huang, S., Yang, W., Wang, J., Yuan, Y., and Yang, S., 2008, Heat flow study at the Chinese Continental Scientific Drilling site: Borehole temperature, thermal conductivity, and radiogenic heat production: Journal of Geophysical Research, v. 113, B02404, p. 1–16, doi: 10.1029/2007jb004958.

Henrys, S., Wilson, T., Whittaker, J., Fielding, C., Hall, J., and Naish, T., 2007, Tectonic history of mid-Miocene to present southern Victoria Land Basin, inferred from seismic stratigraphy in McMurdo Sound, Antarctica, *in* Cooper, A.K., and Raymond, C.R., eds., Antarctica: A Keystone in a Changing World—Online Proceedings of the 10th ISAES: USGS Open-File Report 2007–1047, Research Paper 049.

Hermanrud, C., Cao, S., and Lerche, I., 1990, Estimates of virgin rock temperature derived from BHT measurements: Bias and error: Geophysics, v. 55, no. 7, p. 924–931, doi: 10.1190/1.1442908.

Horgan, H., Naish, T., Bannister, S., Balfour, N., and Wilson, G., 2005, Seismic stratigraphy of the Ross Island flexural moat under the McMurdo-Ross Ice Shelf, Antarctica, and a prognosis for stratigraphic drilling: Global and Planetary Change, v. 45, p. 83–97, doi: 10.1016/j.gloplacha.2004.09.014.

Horner, D.R., 1951, Pressure build-up in wells: The Hague, Proceedings, 3rd World Petroleum Congress, v. 2.

Jarrard, R.D., 2001, Petrophysics of core plugs from the CRP-3 drillhole, Victoria Land Basin, Antarctica: Terra Antartica, v. 8, no. 3, p. 143–150.

Jaupart, C., and Mareschal, J.-C., 2007, Heat flow and thermal structure of the lithosphere, *in* Watts, A.B., ed., Treatise on Geophysics, v. 6, chapter 6: London, Elsevier, p. 217–251.

Jones, F.W., and Pascal, F., 1994, Numerical model calculations of the effects of grain sizes and orientations on the thermal conductivities of composites: Geothermics, v. 23, no. 4, p. 365–371, doi: 10.1016/0375-6505(94)90031-0.

Kreyszig, E., 1983, Advanced Engineering Mathematics: New York, John Wiley and Sons, 344 p.

Krissek, L., Browne, G., Carter, L., Cowan, E., Dunbar, G., McKay, R., Naish, T., Powell, R., Reed, J., Wilch, T., and the ANDRILL-MIS Science Team, 2007, Sedimentology and stratigraphy of the AND-1B core, ANDRILL McMurdo Ice Shelf Project, Antarctica: Terra Antartica, v. 14, no. 3, p. 185–222.

Kyle, P.R., 1990, Erebus Volcanic Province, *in* LeMasurier, W.E., and Thomson, J.W., eds., Volcanoes of the Antarctic Plate and Southern Oceans: Washington, D.C., American Geophysical Union, Antarctic Research Series, v. 48, p. 97–108.

Lachenbruch, A.H., and Brewer, M.C., 1959, Dissipation of the temperature effect of drilling a well in Arctic Alaska: U.S. Geological Survey Bulletin 1083-C, p. 73–109.

Langseth, M.G., 1990, Cooling of deep sea boreholes by circulation and implications for logging techniques in high temperature holes: Scientific Drilling, v. 1, p. 231–237.

Lawson, A.W., Lowell, R., and Jain, A.L., 1959, Thermal conductivity of water at high pressures: The Journal of Chemical Physics, v. 30, p. 643–647, doi: 10.1063/1.1730024.

Lee, T.-C., Duchkov, A.D., and Morozov, S.G., 2003, Determination of thermal properties and formation temperature from borehole thermal recovery data: Geophysics, v. 68, no. 6, p. 1835–1846, doi: 10.1190/1.1635036.

Lovell, M.A., 1985, Thermal conductivities of marine sediments: Quarterly Journal of Engineering Geology, London, v. 18, p. 437–441, doi: 10.1144/GSL.QJEG.1985.018.04.14.

Morin, R., and Silva, A.J., 1984, The effects of high pressure and high temperature on some physical properties of ocean sediments: Journal of Geophysical Research, v. 89, no. B1, p. 511–526, doi: 10.1029/JB089iB01p00511.

Morin, R., Williams, T., Henrys, S., Crosby, T., Hansaraj, D., and the ANDRILL-MIS Science Team, 2007, Downhole measurements in the AND-1B borehole, ANDRILL McMurdo Ice Shelf Project, Antarctica: Terra Antartica, v. 14, no. 3, p. 167–174.

Naish, T., Levy, R., Powell, R., and MIS Science and Operations Team Members, 2006, Scientific Logistics Implementation Plan for the ANDRILL McMurdo Ice Shelf Project: ANDRILL SMO Contribution 7, University of Nebraska-Lincoln, 117 p.

Naish, T., Powell, R., Levy, R., Henrys, S., Krissek, L., Niessen, F., Pompilio, M., Scherer, R., Wilson, G., and the ANDRILL-MIS Science Team, 2007a, Synthesis of the initial scientific results of the MIS Project (AND-1B core), Victoria Land Basin, Antarctica: Terra Antartica, v. 14, no. 3, p. 317–327.

Naish, T., Powell, R., Levy, R., Florindo, F., Harwood, D., Kuhn, G., Niessen, F., Talarico, F., and Wilson, G., 2007b, A record of Antarctic climate and ice sheet history recovered: Eos, Transactions, American Geophysical Union, v. 88, no. 50, p. 557–558, doi: 10.1029/2007EO500001.

Niessen, F., Magens, D., and Gebhardt, A.C., 2007, Physical properties of the AND-1B core, ANDRILL McMurdo Ice Shelf Project, Antarctica: Terra Antartica, v. 14, no. 3, p. 155–166.

Pompilio, M., Dunbar, N., Gebhardt, A.C., Helling, D., Kuhn, G., Kyle, P., McKay, R., Talarico, F., Tulaczyk, S., Vogel, S., Wilch, T., and the ANDRILL-MIS Science Team, 2007, Petrology and geochemistry of the AND-1B core, ANDRILL McMurdo Ice Shelf Project, Antarctica: Terra Antartica, v. 14, no. 3, p. 255–288.

Powell, R.D., Laird, M.G., Naish, T.R., Fielding, C.R., Krissek, L.A., and van der Meer, J.J.M., 2001, Depositional environments for strata cored in CRP-3 (Cape Roberts Project), Victoria Land Basin, Antarctica: palaeoglaciological and palaeoclimatological inferences: Terra Antartica, v. 8, no. 3, p. 207–216.

Pribnow, D.F.C., and Sass, J.H., 1995, Determination of thermal conductivity for deep boreholes: Journal of Geophysical Research, v. 100, no. B6, p. 9981–9994, doi: 10.1029/95JB00960.

Risk, G.F., and Hochstein, R., 1974, Heat flow at Arrival Heights, Ross Island, Antarctica: New Zealand Journal of Geology and Geophysics, v. 17, p. 629–644.

Roy, R.F., Beck, A.E., and Touloukian, Y.S., 1981, Thermophysical properties of rocks, *in* Touloukian, Y.S., Judd, W.R., and Roy, R.F., eds., Physical Properties of Rocks and Minerals: New York, McGraw-Hill, p. 409–502.

Šafanda, J., Heidinger, P., Wilhelm, H., and Čermák, V., 2007, Post-drilling destabilization of temperature profile in borehole Yaxcopoil-1, Mexico: Hydrogeology Journal, v. 15, p. 423–428, doi: 10.1007/s10040-006-0082-8.

Salvini, F., Brancolini, G., Busetti, M., Stroti, F., Mazzarini, F., and Coren, F., 1997, Cenozoic geodynamics of the Ross Sea region, Antarctica: crustal extension, interplate strike-slip faulting and tectonic inheritance: Journal of Geophysical Research, v. 102, B11, p. 24,669–24,696, doi: 10.1029/97JB01643.

Sass, J.H., Lachenbruch, A.H., Moses, T., and Morgan, P., 1992, Heat flow from a scientific research well at Cajon Pass, California: Journal of Geophysical Research, v. 97, p. 5017–5030, doi: 10.1029/91JB01504.

Sass, J.H., Lachenbruch, A.H., and Galanis, S.P., Jr., 1994, Thermal regime of the southern Basin and Range: 1. Heat flow data from Arizona and the Mojave desert of California and Nevada: Journal of Geophysical Research, v. 99, p. 22093–22120, doi: 10.1029/94JB01891.

Sato, S., Asakura, N., Saki, T., Oikawai, N., and Kaneda, Y., 1984, Preliminary results of geological and geophysical surveys in the Ross Sea and in the Dumont d'Urville Sea off Antarctica: Memoirs of the National Institute of Polar Research #33, Proceedings of the 4th Symposium on Antarctic Geosciences, Tokyo, p. 66–92.

Vasseur, G., Brigaud, F., and Demongodin, L., 1995, Thermal conductivity estimation in sedimentary basins: Tectonophysics, v. 244, p. 167–174, doi: 10.1016/0040-1951(94)00225-X.

Villinger, H.W., Langseth, M.G., Gröschel-Becker, H.M., and Fisher, A.T., 1994, Estimating in-situ thermal conductivity from log data: Proceedings of the Ocean Drilling Program: Scientific Results, v. 139, p. 545–552.

Watson, T., Nyblade, A., Wiens, D.A., Anandakrishnan, S., Benoit, M., Shore, P.J., Voigt, D., and VanDecar, J., 2006, P and S velocity structure of the upper mantle beneath the Transantarctic Mountains, East Antarctic craton, and Ross Sea from travel time tomography: Geochemistry Geophysics Geosystems, v. 7, no. 7, p. 1–17, doi: 10.1029/2005GC001238.

White, P., 1989, Downhole logging, *in* Barrett, P.J., ed., Antarctic Cenozoic History from the CIROS-1 Drillhole, McMurdo Sound: Wellington, Department of Scientific and Industrial Research Bulletin, p. 7–14.

Williams, T., Morin, R., Jackolski, C., Jarrard, R., Henrys, S., Niessen, F., Magens, D., and Powell, R., 2008, The record of paleoenvironmental change at the ANDRILL McMurdo Ice Shelf site, Antarctica, from downhole measurements: Oslo, Norway, International Geological Congress, Abstract AAN-027.

Wilson, T.J., 1999, Cenozoic structural segmentation of the Transantarctic Mountains rift flank in southern Victoria Land, Antarctica, *in* van der Wateren, F.M., and Cloetingh, S., eds., Lithosphere Dynamics and Environmental Change of the Cenozoic West Antarctic Rift System: Global and Planetary Change, v. 23, no. 1–4, p. 105–127.

Woodside, W., and Messmer, J.H., 1961, Thermal conductivity of various rocks, I Unconsolidated sands, II Consolidated rocks: Journal of Applied Physics, v. 32, p. 1688–1706, doi: 10.1063/1.1728419.

Yusufova, V.D., Pepinov, R.I., Nicolayev, V.A., Zokhrabbekova, G.U., Lubcova, N.V., and Tuayev, T.D., 1978, Thermophysical properties of softened seawater and salt solutions over a wide temperature and pressure range: Desalination, v. 25, p. 269–280, doi: 10.1016/S0011-9164(00)80326-4.

Zemanek, J., Glenn, E.E., Norton, L.J., and Caldwell, R.L., 1970, Formation evaluation by inspection with the borehole televiewer: Geophysics, v. 35, p. 254–269, doi: 10.1190/1.1440089.

Manuscript Received 16 March 2009
Revised Manuscript Received 02 November 2009
Manuscript Accepted 15 December 2009